

# Measurements and coupled reaction channels analysis of one- and two-proton transfer reactions for the $^{28}\text{Si} + ^{90,94}\text{Zr}$ systems

Sunil Kalkal,<sup>1,\*</sup> S. Mandal,<sup>1</sup> A. Jhingan,<sup>2</sup> J. Gehlot,<sup>2</sup> P. Sugathan,<sup>2</sup> K. S. Golda,<sup>2</sup> N. Madhavan,<sup>2</sup> Ritika Garg,<sup>1</sup> Savi Goyal,<sup>1</sup> Gayatri Mohanto,<sup>2</sup> Rohit Sandal,<sup>3</sup> Santosh Chakraborty,<sup>4</sup> Shashi Verma,<sup>1</sup> Bivash Behera,<sup>3</sup> G. Eleonora,<sup>5</sup> H. J. Wollersheim,<sup>5</sup> and R. Singh<sup>1,6</sup>

<sup>1</sup>*Department of Physics & Astrophysics, University of Delhi, Delhi, India*

<sup>2</sup>*Inter University Accelerator Center, New Delhi, India*

<sup>3</sup>*Department of Physics, Panjab University, Chandigarh, India*

<sup>4</sup>*Saha Institute of Nuclear Physics, Calcutta, India*

<sup>5</sup>*GSI, D-64291 Darmstadt, Germany*

<sup>6</sup>*AINST, Amity University, Noida, India*

(Received 14 December 2011; revised manuscript received 17 February 2012; published 15 March 2012)

Measurements of angular distributions for one- and two-proton stripping reactions for  $^{28}\text{Si} + ^{90,94}\text{Zr}$  systems were performed at 120 MeV. The experiment was carried out with the  $^{28}\text{Si}$  beam at Inter University Accelerator Center, New Delhi. The theoretical calculations were performed using the quantum mechanical coupled reaction channels code FRESKO. The distorted wave Born approximation calculations reproduced the experimental angular distributions for the one-proton transfer channel for both the systems reasonably well but failed for the two-proton transfer channel. Coupled channels calculations including various intermediate states (involving target and projectile inelastic excitations before and/or after transfer) along with the sequential transfer were able to reproduce the two-proton transfer angular distributions for both the systems reasonably well. It seems that at an energy above the Coulomb barrier, there is significant contribution of the indirect multistep and sequential transfer to the two-proton stripping reaction.

DOI: [10.1103/PhysRevC.85.034606](https://doi.org/10.1103/PhysRevC.85.034606)

PACS number(s): 25.70.Hi, 24.10.Eq

## I. INTRODUCTION

Transfer reactions have been an intriguing subject of study for the last few decades for various reasons. These reactions were initially used for spectroscopic studies mainly with light ions [1–3]. The reaction mechanism with light ions is much simpler as compared to that with the heavy ions. Transfer reactions with heavy ions are also useful to study the nucleon correlation effects on the nucleus [4] and its effect on the reaction mechanism. There has been a renewed interest in these reactions for the production and structure studies of the nuclei near the drip lines [5,6]; mainly the neutron-rich nuclei. The multinucleon transfer reactions can take place either sequentially or simultaneously and the number of such possibilities increases drastically with an increasing number of transferred nucleons. Inelastic excitations of the projectile and the target before or after the transfer further complicate the process. The inclusion of these processes in the theoretical codes and the establishment of the reaction mechanism is a very intricate procedure [4,7–9].

One-nucleon transfer reactions are very well described with the distorted wave Born approximation (DWBA) formalism using the optical model potential. This formalism, however, fails to describe the two-nucleon transfer data where the sequential or successive transfer of nucleons plays an important role [10]. The DWBA formalism assumes one-step transfer from the ground states of the interacting nuclei directly to the

specified states of the outgoing nuclei. So, the DWBA is not an appropriate approach when the nuclei in the incident channel are excited or the transfer of nucleons takes place via multistep processes, which is a very likely mechanism in the heavy-ion transfer reactions. The heavy-ion transfer reactions are well described by the coupled reaction channels theory [11] where all the possibilities are taken into account.

In this paper we investigate the relative importance of the simultaneous and sequential transfer using the coupled reaction channels (CRC) formalism for  $^{28}\text{Si} + ^{90,94}\text{Zr}$  systems at an energy above the Coulomb barrier ( $E_{\text{lab}} = 120$  MeV). We have already carried out the transfer measurements for these systems at the sub- and near-barrier energies [12]. The Coulomb barriers for  $^{28}\text{Si} + ^{90,94}\text{Zr}$  systems are 95.8 and 94.2 MeV, respectively, in the laboratory frame. Theoretical calculations were performed using a quantum mechanical code based on the CRC formalism FRESKO [13]. A comparison has been made between the results obtained from the DWBA and CRC calculations for one- and two-proton transfer channels.

The paper is organized as follows. The next section gives the experimental details. In Sec. III, the experimental angular distributions for one- and two-proton transfer channels for  $^{28}\text{Si} + ^{90,94}\text{Zr}$  systems are compared with the theoretical calculations carried out in the DWBA framework and the CRC formalism. In Sec. IV, the summary and conclusion are presented.

## II. EXPERIMENTAL DETAILS

The experiment was performed with a  $^{28}\text{Si}$  beam at a laboratory energy of 120 MeV ( $\sim 25$  MeV above the barrier)

\*Present address: Indiana University, South Bend, Indiana; [kalkal84@gmail.com](mailto:kalkal84@gmail.com)

in a general purpose scattering chamber (GPSC) at Inter University Accelerator Center (IUAC), New Delhi. The targets used were isotopically enriched  $^{90,94}\text{Zr}$  (97.65% and 96.07%, respectively)  $280\ \mu\text{g}/\text{cm}^2$  thick foils prepared on  $45\ \mu\text{g}/\text{cm}^2$  carbon backings [14]. The scattering chamber with an inner diameter of 1.5 m is equipped with two movable arms which can be rotated externally without breaking the vacuum. Two monitors were placed at angles of  $\pm 10^\circ$  with respect to the beam direction for beam monitoring as well as normalization to extract the transfer reaction cross sections. On the left arm of the GPSC, a multiwire proportional counter (MWPC) with an active area of  $5 \times 5\ \text{cm}^2$  was placed at a distance of 37.5 cm followed by an ionization chamber (IC) with an active volume of  $8 \times 4.5 \times 21\ \text{cm}^3$ , for the detection of the projectilelike transfer products. On the right arm an MWPC with an active area of  $5 \times 5\ \text{cm}^2$ , was placed at a distance of 60 cm for the detection of the targetlike transfer products. The MWPC cathode and anode were biased to  $-160\ \text{V}$  and  $+410\ \text{V}$ , respectively. The angular resolution of the MWPCs was found to be  $0.05^\circ$  using an  $^{241}\text{Am}$  alpha source placed at a distance of 60 cm. The isobutane gas was circulated continuously in the MWPCs at a pressure of 3 mbar. The gas pressure in the IC was adjusted in such a way that the particles lost approximately 60% of their energies in the first two segments to get the best possible particle separation. The energy resolution of the IC was 120 keV with 5.48 MeV alphas from the  $^{241}\text{Am}$  source. Figure 1 shows a schematic of the experimental setup. The angular distribution measurements of the transfer reaction products were performed around the grazing angle ( $\theta_{\text{gr}} \sim 66^\circ$ ) at  $42^\circ$ ,  $50^\circ$ ,  $58^\circ$ ,  $66^\circ$ ,  $72^\circ$ ,  $78^\circ$  angles for the projectilelike transfer products. The other arm was rotated to the corresponding angles for the detection of the targetlike particles. A kinematic coincidence was set up between the MWPCs on the two arms. Time of flight (TOF) was set up in the hardware using a TAC with the arrival of projectilelike particles in the left MWPC as start, and a signal of the right MWPC used for the detection of targetlike particles as stop. In the TOF spectrum, apart from this peak, two other peaks, one arising from the targetlike particles in the left detector as start and the projectilelike particles in the right detector as stop and the second arising from the carbon backing

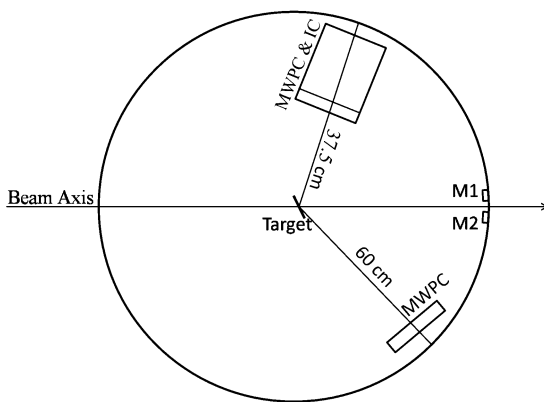


FIG. 1. A schematic of the experimental setup used for the measurement of transfer products angular distributions at 120 MeV for  $^{28}\text{Si} + ^{90,94}\text{Zr}$  systems.

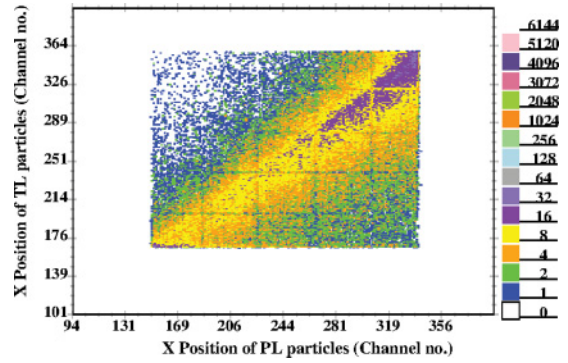


FIG. 2. (Color online) A two-dimensional spectrum showing the position (angular) correlation between the projectilelike (PL) and the targetlike (TL) particles at  $66^\circ$  for  $^{28}\text{Si} + ^{90}\text{Zr}$  system.

were observed. The delays were adjusted to maximize the transfer peak events. At the same time, a very good one-to-one correspondence, shown in Fig. 2, was observed in the positions of the particles detected in the two MWPCs. The position correlation spectrum is actually the angle correlation spectrum. The intensity of the peak falls from one edge to the other as the elastic scattering cross section starts decreasing rapidly around and after  $66^\circ$  at this energy. The coincidence between the two MWPCs was also very helpful in separating the alpha transfer channel from the two-proton transfer channels because of the difference in the kinematics. We could clearly resolve the nuclei with different  $Z$  values by using the IC. Figure 3 shows a two-dimensional spectrum of  $E_2$  (energy lost by the particles in the second segment of the IC) versus total energy ( $E$ ) deposited in the IC for the  $^{28}\text{Si} + ^{94}\text{Zr}$  system.

### III. RESULTS AND DISCUSSION

The elastic scattering data were normalized to the theoretical calculations using FRESKO at the forward angles and the resulting normalization constant was used for extracting the transfer reaction cross sections. The two-dimensional particle identification spectrum obtained from the IC was linearized and gated by TOF defined between the MWPCs to accept the coincidence events only. This gated spectrum was then

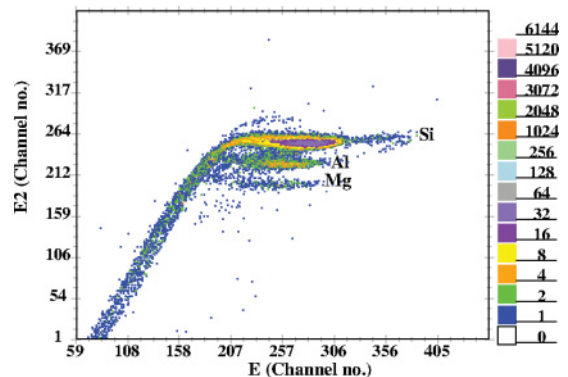


FIG. 3. (Color online) A two-dimensional spectrum of energy lost in the second section versus total energy deposited in IC by projectilelike particles at  $66^\circ$  for the  $^{28}\text{Si} + ^{94}\text{Zr}$  system at 120 MeV.

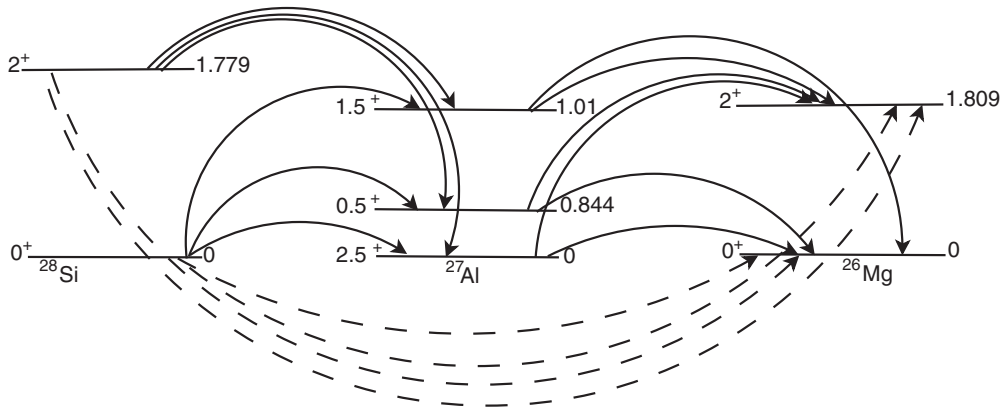


FIG. 4. A schematic of the couplings of the projectilelike nuclei included in the calculations for both the systems. The continuous lines are for sequential transfer whereas the dashed lines are for simultaneous transfer. The energies of the states are in MeV.

projected on to the  $y$  axis to get the transfer events. The differential cross sections for these channels were extracted at each angle by normalizing with respect to the monitor detectors using the formula,

$$\frac{\sigma_{\text{Transfer}}}{\sigma_{\text{MON}}} = \frac{\left(\frac{d\sigma}{d\Omega}\right)_{\text{Transfer}}(\Delta\Omega)_{\text{MWPC}}}{\sigma_{\text{MON}}} = \frac{Y_{\text{MWPC}}}{Y_{\text{MON}}}, \quad (1)$$

where  $Y_{\text{MWPC}}$  is the number of particles detected in the MWPC for a particular transfer channel,  $Y_{\text{MON}}$  is the geometric mean of the monitor counts,  $\sigma_{\text{Transfer}}$  is the transfer cross section of the particular channel,  $\left(\frac{d\sigma}{d\Omega}\right)_{\text{Transfer}}$  is the differential transfer cross section at an angle where MWPC is placed, and  $\Delta\Omega_{\text{MWPC}}$  is the solid angle subtended by the MWPC at the target. As the monitors were placed at  $\pm 10^\circ$ , the elastic cross section  $\sigma_{\text{MON}}$  was taken to be the same as the Rutherford scattering (theoretically,  $\sigma_{\text{elastic}}/\sigma_{\text{Rutherford}} \sim 1$  at this angle.)

Angular distributions for the one- and two-proton stripping channels were analyzed using the code FRESKO. The calculations were performed in both the DWBA and the CRC frameworks using this code. The schematics of couplings used in the calculations are drawn in Figs. 4–6 for all the nuclei. The

Akyuz Winther (AW) parametrization [15] was used for the optical model parameters. A list of the various potential parameters used in the calculations is given in Table I. In the CRC transfer calculations, we have used finite range approximation for the transfer channels and the full remnant terms were also taken into account. The calculations were performed taking the interaction potential prior to the transfer. The higher order multistep transfer processes involving inelastic excitations of the target and the projectile before or after the reaction were also included while performing the CRC calculations. The Coulomb radius parameter was assumed to be  $r_{0c} = 1.25$  fm. The same values of the AW potential parameters were used in the calculations for the fusion excitation functions [16] using CCFULL [17] and the transfer reactions using FRESKO for these systems. The standard form of spin-orbit potential was used in the calculations. A sufficiently large number of the partial waves ( $l_{\text{max}} = 250\hbar$ ) were used in the calculations.

For one- and two-proton transfer calculations, the Woods-Saxon shapes of the real potentials were used for  $^{27}\text{Al} + 1p$ ,  $^{26}\text{Mg} + 2p$ ,  $^{90}\text{Zr} + 1p$ ,  $^{90}\text{Zr} + 2p$ ,  $^{94}\text{Zr} + 1p$ ,  $^{94}\text{Zr} + 2p$  with

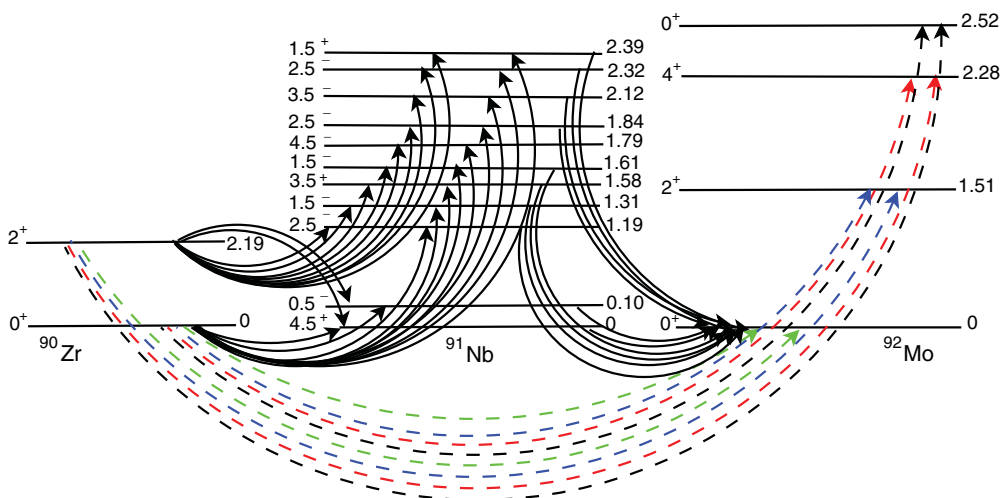


FIG. 5. (Color online) A schematic of the couplings of the targetlike nuclei included in the calculations for  $^{28}\text{Si} + ^{90}\text{Zr}$  system. The continuous lines are for the sequential transfer whereas the dashed lines are for the simultaneous transfer. The energies of the states are in MeV.

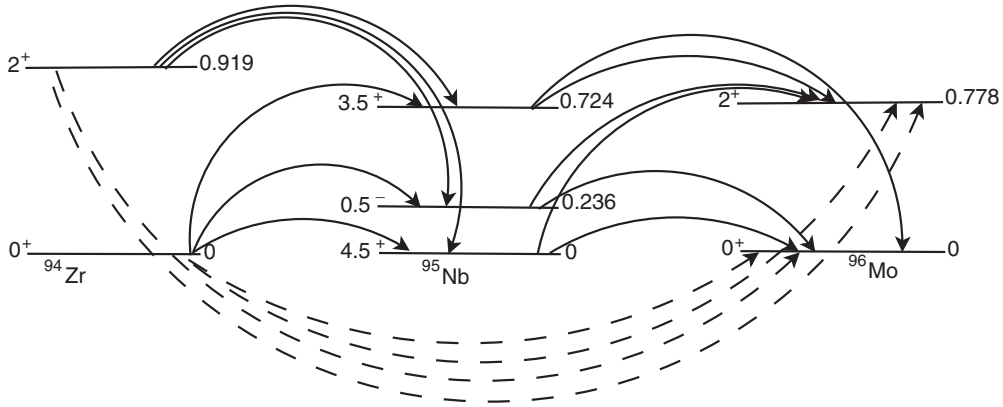


FIG. 6. A schematic of the couplings of the targetlike nuclei included in the calculations for the  $^{28}\text{Si} + ^{94}\text{Zr}$  system. The continuous lines are for the sequential transfer whereas the dashed lines are for the simultaneous transfer. The energies of the states are in MeV.

realistic diffuseness ( $a_0 = 0.60$  fm) and radius ( $r_0 = 1.16$  fm) parameters. The strength of the real potential ( $V_0$ ) for these channels was adjusted to reproduce one- and two-proton separation energies for both the systems. The values of the parameters for the imaginary potential were,  $W_0 = 50$  MeV,  $r_w = 1.0$  fm,  $a_w = 0.4$  fm, with Woods-Saxon shape. In FRESKO, the relative strength of the inelastic couplings is the reduced matrix element for the Coulomb transitions and it is the reduced deformation length for nuclear transitions. For a transition of multipole  $k$  from initial state  $I$  to final state  $I'$ , the reduced matrix element is given by

$$M(Ek, I \rightarrow I') = \pm \sqrt{(2I+1)B(Ek, I \rightarrow I')}, \quad (2)$$

whereas the reduced nuclear deformation length is given by

$$RDEF(k, I \rightarrow I') = M(Ek) \times \frac{4\pi}{[3ZR^{k-1}]}. \quad (3)$$

The values of the relative strengths used in the calculations are given in Table II. The values of  $B(Ek)$  given in this table are taken from Refs. [18, 19]. The spectroscopic factor (taken to be one for some states because of unavailability), the interaction potential for transfer process, the detailed structure of the projectile or target in the calculation, the form factor, and the choice of the optical potential can affect the theoretical calculations and hence, the calculations had to be normalized. The obtained theoretical results were normalized (by a factor of  $\sim 1.5$ – $4.3$ ) to give the best description of the experimental data for both the systems.

Figure 7 shows the experimental results of the one-proton stripping channel along with the FRESKO calculations for the  $^{28}\text{Si} + ^{90}\text{Zr}$  system. As expected, the differential transfer cross section was peaking around the grazing angle. An

TABLE I. The parameters of the AW potential (Woods-Saxon form) used in the coupled reaction channels calculations using the code FRESKO.

System	$V_0$ (MeV)	$r_0$ (fm)	$a$ (fm)
$^{28}\text{Si} + ^{90}\text{Zr}$	66.01	1.176	0.659
$^{28}\text{Si} + ^{94}\text{Zr}$	66.49	1.176	0.660

oscillatory behavior was observed at the forward angles in theoretical calculations which might be from the interference effects, as for a certain angle, there might be scattering from the different impact parameters giving the same deflection angle [6]. Quantum mechanically, the oscillations may be attributed to the diffraction phenomenon. A reasonably good agreement was obtained between the theoretically calculated and the experimentally observed angular distributions. The one-step DWBA calculations were also performed which could reproduce the trend of the data reasonably well.

The two-proton stripping angular distribution along with full coupled reaction channels calculations and one-step DWBA calculations are shown in Fig. 8 for the  $^{28}\text{Si} + ^{90}\text{Zr}$  system. A comparatively broad angular distribution was observed for the two-proton stripping channel. While performing the theoretical calculations sequential transfer including various intermediate states as well as one-step direct transfer were taken into account in the coupling scheme. Theoretical coupled channels calculations including sequential and simultaneous transfer reproduced the data reasonably well, but the one-step DWBA failed to do so as it assumes that the two nucleons are transferred simultaneously as a cluster directly from the initial state to the final state. A large number of the  $^{91}\text{Nb}$  states had significant transfer cross sections (states until the cross section reduced by an order of magnitude compared to that of the most populated state) and hence, were included in the FRESKO calculations.

TABLE II. Electromagnetic matrix elements and reduced deformation lengths for nuclear transitions ( $\delta_N$ ) and the reduced matrix element for Coulomb transitions ( $\delta_c$ ) for various nuclei used in FRESKO calculations.

States	$\langle I'    Ek    I \rangle (e^2 b^k)$	$\delta_N$	$\delta_c$
$^{90}\text{Zr}(2^+ \rightarrow 0^+)$	0.061	0.481	24.7
$^{90}\text{Zr}(3^- \rightarrow 0^+)$	0.098	1.133	313
$^{94}\text{Zr}(2^+ \rightarrow 0^+)$	0.066	0.493	25.7
$^{94}\text{Zr}(3^- \rightarrow 0^+)$	0.090	1.101	300
$^{28}\text{Si}(2^+ \rightarrow 0^+)$	0.033	1.482	18.0
$^{28}\text{Si}(3^- \rightarrow 0^+)$	0.004	1.460	64.8

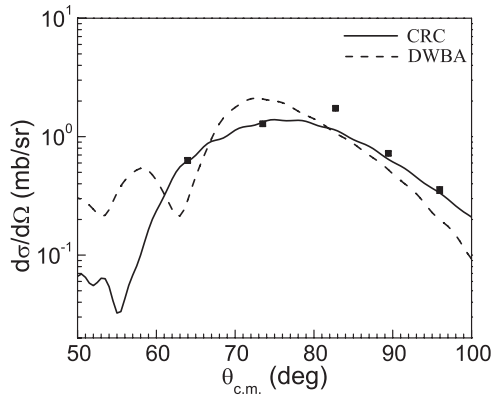


FIG. 7. The experimental angular distribution for the one-proton stripping channel for the  $^{28}\text{Si} + ^{90}\text{Zr}$  system along with the corresponding theoretical calculations using FRESKO.

The experimental angular distribution for the one-proton stripping channel for  $^{28}\text{Si} + ^{94}\text{Zr}$  system is shown in Fig. 9. The theoretical calculations with full coupled reaction channels and the one-step DWBA are also shown in this figure. As observed in the case of  $^{28}\text{Si} + ^{90}\text{Zr}$  also, the one-step DWBA calculations predicted the angular distribution of the one-proton transfer channel reasonably well. For this system also, theoretical calculations predicted an oscillatory behavior at the forward angles. This kind of behavior is generally observed at energies above the Coulomb barrier as at these energies, there can be more than one impact parameter which scatter on to the same angle.

In Fig. 10, the experimental differential cross sections and the full CRC calculations along with simultaneous and the sequential transfer contributions are shown for the two-proton stripping channel for the  $^{28}\text{Si} + ^{94}\text{Zr}$  system. From the theoretical calculations using FRESKO, it is observed that at energies above the barrier the simultaneous and the sequential transfer of protons contribute equally to the measured cross sections around the grazing angle but the simultaneous transfer starts dominating at large angles. The correlated pair transfer was observed to be a significant mechanism for neutron transfer in the sub-barrier region for these systems [12] and for proton transfer in the  $^{16}\text{O} + ^{208}\text{Pb}$  system [20].

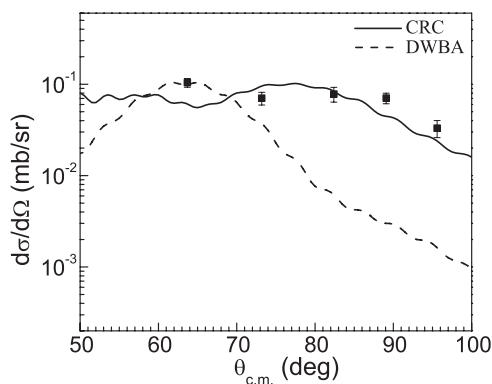


FIG. 8. The experimental angular distribution for the two-proton stripping channel for the  $^{28}\text{Si} + ^{90}\text{Zr}$  system along with the DWBA and CRC calculations using FRESKO.

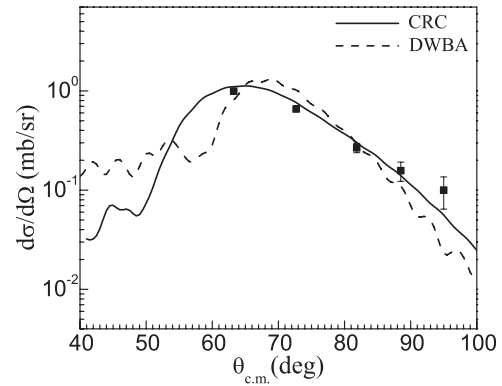


FIG. 9. The experimental angular distribution for the one-proton stripping channel for the  $^{28}\text{Si} + ^{94}\text{Zr}$  system along with the corresponding theoretical calculations using FRESKO.

It is to be noted that the angular distributions for the two-proton stripping were much broader than those for the one-proton stripping in both the systems and no peaking was observed at the grazing angle in the two-proton stripping channel which was very well observed experimentally and predicted theoretically, by both full CRC calculations as well as the one-step DWBA calculations in the case of one-proton stripping for both the systems. The broader angular distributions may be explained in terms of indirect transfer (involving inelastic excitation of the colliding nuclei) [6] or the sequential mechanism which contributes significantly to the indirect transfer. The two-step contribution (transfer followed by inelastic excitation or the inelastic excitation followed by transfer) gives rise to broad angular distribution. The interference between the direct (no inelastic excitation involved) and the indirect transfer affects the magnitude of the cross section and the shape of the angular distribution.

#### IV. SUMMARY AND CONCLUSION

The angular distributions of one- and two-proton stripping reactions have been measured for  $^{28}\text{Si} + ^{90,94}\text{Zr}$  systems at

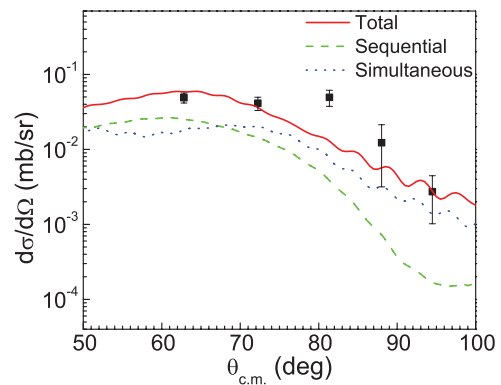


FIG. 10. (Color online) The experimental angular distribution for the two-proton stripping channel for the  $^{28}\text{Si} + ^{94}\text{Zr}$  system along with the corresponding theoretical calculations using FRESKO. The contribution of the sequential and simultaneous transfer are shown as dashed and dotted lines, respectively.

an energy ( $E_{\text{Lab}} = 120$  MeV) above the barrier. The CRC calculations have been performed taking into account the exact finite range effects in transfer reactions using FRESKO. The Akyuz-Winther parametrization of the optical model for the real potential was used. A short-range imaginary potential was used to take the absorption of the flux into account. It was found that the DWBA calculations could describe the one-proton transfer data reasonably well for both the systems but failed to reproduce the angular distribution for the two-proton transfer. The CRC calculations including various intermediate states and the excitations of the projectile (target) before or after the reaction could reproduce the angular distributions for one- as well as two-proton transfer channels for both the systems reasonably well. This lends support to the multistep transfer to

be playing an important role at energies much above the barrier. Some more multinucleon (proton as well as neutron) transfer measurements in different energy regions should prove quite useful to fully understand this kind of behavior.

#### ACKNOWLEDGMENTS

We are thankful to the Pelletron staff of the IUAC for providing a stable beam. We are indebted to the target laboratory staff of the IUAC, especially S. R. Abhilash, for the help in the preparation of good quality isotopic targets. One of the authors (S.K.) gratefully acknowledges the support from Council of Scientific & Industrial Research, New Delhi.

- 
- [1] R. G. Clarkson and W. R. Coker, *Phys. Rev. C* **2**, 1108 (1970).
  - [2] E. R. Flynn, F. Ajzenberg-Selove, R. E. Brown, J. A. Cizewski, and J. W. Sunier, *Phys. Rev. C* **24**, 2475 (1981).
  - [3] P. O. Soderman *et al.*, *Nucl. Phys. A* **587**, 55 (1995).
  - [4] W. Von Oertzen and A. Vitturi, *Rep. Prog. Phys.* **64**, 1247 (2001).
  - [5] H. Lenske and G. Schrieder, *Eur. Phys. J. A* **2**, 41 (1998).
  - [6] Yu. E. Penionzhkevich, G. G. Adamian, and N. V. Antonenko, *Phys. Lett. B* **621**, 119 (2005).
  - [7] C. Y. Wu, W. Von Oertzen, D. Cline, and M. W. Guidry, *Annu. Rev. Nucl. Part. Sci.* **40**, 285 (1990).
  - [8] W. R. Philips, *Rep. Prog. Phys.* **40**, 345 (1977).
  - [9] L. Corradi, G. Pollarolo, and S. Szilner, *J. Phys. G* **36**, 113101 (2009).
  - [10] P. P. Tung, K. A. Erb, M. W. Sachs, G. B. Sherwood, R. J. Ascutto, and D. A. Bromley, *Phys. Rev. C* **18**, 1663 (1978).
  - [11] G. R. Satchler, *Direct Nuclear Reactions* (Oxford University Press, Oxford, 1983).
  - [12] Sunil Kalkal *et al.*, *Phys. Rev. C* **83**, 054607 (2011).
  - [13] Ian J. Thompson, *Comput. Phys. Rep.* **7**, 167 (1988).
  - [14] Sunil Kalkal *et al.*, *Nucl. Instrum. Methods Phys. Res., Sect. A* **613**, 190 (2010).
  - [15] R. A. Broglia and A. Winther, *Heavy Ion Reaction Lecture Notes, Volume 1: Elastic and Inelastic Reactions* (Benjamin/Cummings, Reading, 1981).
  - [16] Sunil Kalkal *et al.*, *Phys. Rev. C* **81**, 044610 (2010).
  - [17] K. Hagino, N. Rowley, and A. T. Kruppa, *Comput. Phys. Commun.* **123**, 143 (1999).
  - [18] S. Raman, C. W. Nestor Jr., and P. Tikkanen, *At. Data Nucl. Data Tables* **78**, 1 (2001).
  - [19] T. Kibedi and R. H. Spear, *At. Data Nucl. Data Tables* **80**, 35 (2002).
  - [20] M. Evers, M. Dasgupta, D. J. Hinde, D. H. Luong, R. Rafiei, R. duRietz, and C. Simenel, *Phys. Rev. C* **84**, 054614 (2011).